14

Aortic, Renal, and Carotid CT Angiography

Matthew J. Budoff

Introduction

Volumetric datasets acquired with very thin slices (anywhere from 0.625 to 1.5 mm per image) will allow visualization of smaller structures with less partial volume averaging in the *z*-axis as well as superior 3-D and/or multiplanar imaging. Newer multidetector CT (MDCT) scanners have near isotropic voxels (similar *z*-axis to *x*-axis and *y*-axis imaging resolution), which results in improved multiplane reconstructions with higher resolution.

Computed tomographic angiography of other vascular beds is significantly easier to perform and interpret than coronary studies. There is no cardiac motion to contend with, so gating is most often not necessary. The exception is the ascending aorta, where pseudodissections have plagued earlier studies with single slice CT, due to motion artifacts [1]. Non-gated modes allow for very fast acquisition, and interpretation is significantly less complicated. Most of the large vessels of interest (carotid, renal, mesenteric) have significantly larger diameters than those of coronary arteries, as well as less tortuous courses. Renal and carotid arteries are usually straight structures, so reconstructions are significantly less complicated than coronary imaging. Also, due to the increased speed of newer systems (electron beam tomography and 16+ row multidetector computed tomography), venous enhancement is less common, so it is easier to see the arteries without superimposed contrast-filled structures. This is another reason why CT is most often superior to magnetic resonance imaging in these other vascular beds. Of course, the requirements of radiation (more significant for carotid imaging due to radiation-sensitive organs such as thyroid and orbits) and contrast (more significant for renal artery imaging due to the frequent coexistence of renal insufficiency and renal artery stenosis) make magnetic resonance more attractive for selective cases. In regard to the aorta, CT angiography can diagnose aneurysm, dissection, and wall abnormalities such as ulceration, calcification, or thrombus throughout the full length of the aorta as well as involvement of branch vessels.

Disease of the aorta or great vessels can present with a broad clinical spectrum of symptoms and signs. The accepted diagnostic gold standard, selective digital subtraction angiography, is now being challenged by state-of-the-art CT angiography (CTA) and MR angiography (MRA). Currently, in many centers, cross-sectional imaging modalities are being used as the first line of diagnosis to evaluate the cardiovascular system, and conventional angiography is reserved for therapeutic intervention.

Principles of Imaging

In aortic imaging, the volume coverage capabilities of MDCT come to full use without having to compromise on resolution of detail [2,3]. With the current configuration of 16-row (or greater) CT scanners, the entire abdominal aorta and the iliac arteries can be covered within seconds and with isotropic resolution (Chapter 1). Interrogation of the dataset can now be made in the anteroposterior (coronal) and lateral (sagittal) planes, which has been the convention with invasive angiography.

Larger collimation (more detectors) reduces contrast, as the imaging territory is covered in a shorter period of time. Another technique to minimize contrast is use of saline to flush the contrast through the system (Chapter 2). The saline chaser offers two significant benefits with CTA imaging. One is that the contrast is forced from the tubing and extremity veins into the central circulation, allowing for a reduction in the total dose of contrast. A second benefit is that the contrast sitting in the vein during imaging can cause partial volume (beam hardening) artifacts. Moving the contrast out of the venous system is important for cardiac imaging (where the scatter from the superior vena cava can cause artifacts in the right atrium and right coronary artery), carotid imaging (obscuring the

proximal brachiocephalic artery or carotid base), and pulmonary imaging.

CT Technique

Understanding the principles of CTA techniques is essential to acquire diagnostic images consistently. This section reviews current CTA methods used in the evaluation of great vessels. The following broad approach is a guide to CT scan acquisition for various scanners.

1. Intravenous injection of 75–150 mL of a non-ionic contrast agent (300–370 mg I/mL), although decreasing with scanners with higher detectors.
2. Monophasic or biphasic injection rate: most commonly a monophasic injection at 4 mL/s (followed by a saline bolus).
3. Scan delay determined by test injection (10 mL at 4 mL/s) or by automated triggering (to achieve imaging to coincide with contrast arrival in the aortic root).
4. Pitch:
   - *For 4-row MDCT*: 4 × 2.50 mm detector configuration with 2.50 mm reconstruction thickness and pitch = 1.4 (table speed 14 mm/rotation, divided by 10 mm detector width), rotation speed 0.5 seconds, reconstructed at 1.00–1.25 mm interval for 3-D and MPR.
   - *For 8-row MDCT*: 8 × 1.25 mm detector configuration with 1.25–2.50 mm reconstruction thickness and pitch = 1.7 (table speed 16.8 mm/rotation divided by 10 mm detector width) during the arterial phase, reconstructed at 0.5–1.25 mm intervals for 3-D and MPR.
   - *For 16-detector MDCT*: 16 × 0.625 mm detector configuration with 1.25–2.50 mm reconstruction thickness and pitch = 1.7 (table speed 17.5 mm/rotation divided by 10 mm detector width), reconstructed retrospectively with 0.3 mm interval for 3-D and MPR
   - *For 64-detector MDCT*: 64 × 0.625 mm detector configuration* with 1.25–2.50 mm reconstruction thickness and pitch = 1.375 (table speed 55 mm/rotation divided by 40 mm detector width), reconstructed retrospectively with 0.3 mm interval for 3-D and MPR. (The 40 mm of detector width coverage per rotation used is currently available in the GE and Phillips systems. Siemens has 20 mm of collimation with the 64-MDCT scanner, with Toshiba allowing 32 mm of coverage per rotation (2005)).

Electron beam tomography (EBT) is performed by use of the continuous volume mode, whereby the scanner simulates the MDCT by taking continuous images of the volume of interest, without gating or pause. In this mode, the scanner can take 10 images per second, covering 1.5 mm to 6 mm per slice. Thus, large areas can be scanned with minimal contrast use. The most common protocols employed increase the image acquisition time from 100 ms per image to 200–300 ms per image, to improve tissue penetration and reduce image noise. Still, approximately 80 mL of contrast is all that is necessary to complete a thoracic and abdominal aortic study.

Aortic Imaging

The speed and ease of modern CTA make it the technique of choice for diagnosing chronic and acute aortic pathologic findings such as intramural hematoma, aneurysm, traumatic injuries, and dissection (Figure 14.1). With the current configuration of 16-row CT scanners, the entire abdominal aorta and the iliac arteries can be covered with isotropic resolution. Moreover, the high scan speed allows substantial reduction of the amount of contrast material used in earlier studies.

Aortic Dissection

The superior temporal resolution of EBT or MDCT significantly improves imaging of the aorta, because motion artifacts are eliminated in the ascending aorta. CT is often considered a superior method over other imaging methods for identification of aortic dissection (even invasive angiography in some cases), as the intimal flap is usually well delineated, even in branches of the aorta. The ability to visualize the great vessels into the transverse

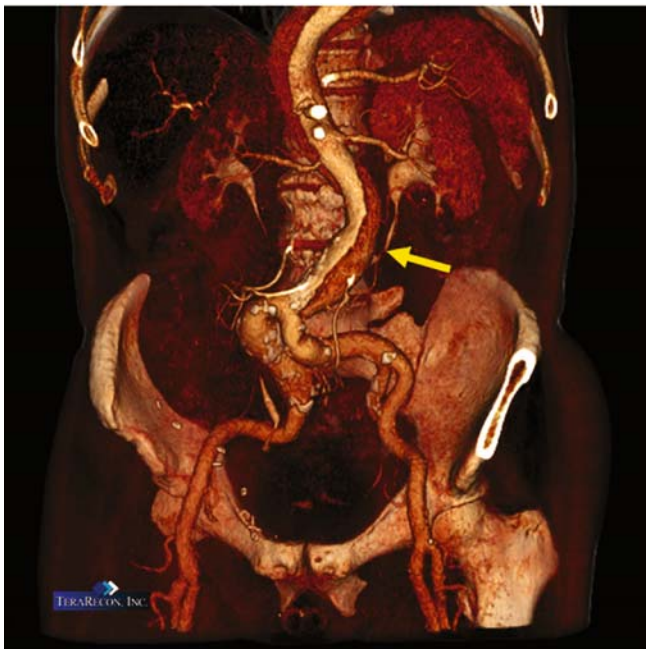

Figure 14.1. A volume-rendered image depicting an aortic dissection involving the abdominal aorta (arrow), starting below the renal arteries and ending prior to the iliac arteries. (Courtesy of TeraRecon, Inc.)

aorta, neck, and arms makes CT significantly more robust than transesophageal imaging and significantly better tolerated by patients. Because imaging protocols are less than 10 minutes (significantly shorter than MR or transesophageal echocardiography), even unstable patients can be evaluated and triaged quickly. With EBT, the flow mode also allows for assessing luminal flow in the true and false lumens.

Thoracic Imaging

CT is the primary means of imaging the lung, thoracic trauma (blunt and penetrating), aneurysms, and aortic dissections [4]. CT is playing an increasingly important role in the diagnosis and management of thoracic aortic pathology [5,6]. In the situation of an acute life-threatening event, CT can provide extensive information concerning the heart, aorta, and great vessels with a single scan protocol (Figure 14.2). In addition, during the same examination, the brain and spinal canal can be evaluated, if necessary. The entire global CT examination (head, cervical spine, chest, abdomen, and pelvis) can be completed on modern MDCT systems in less than 15 minutes [7].

Thoracic aortic imaging is the one area where gating to the cardiac cycle (similar to coronary CTA applications) is important [8]. The reduction in motion artifact provided by ECG gating is especially relevant to axial data from the ascending aorta. The evaluation of aneurysms of the ascending thoracic aorta and in the assessment of possible type A aortic dissection is improved with this methodology due to effective elimination of motion artifacts [9]. Moreover, the possibility of applying ECG-controlled X-ray tube dose modulation is an authentic step forward for reducing radiation exposure rates.

Comparison to Other Methods

Although MRI and transesophageal echocardiography can provide exquisite and unique information, the robust nature of CT often makes it the imaging modality of choice. Advantages are the ability to image the entire aorta and beyond, demonstration of surrounding structures and organs, quantitative measures of aneurysm size and location, and a rapid examination time. Limitations are the negative effects of iodinated contrast on renal function, the rare adverse reactions to iodinated contrast, and the inability to directly measure blood flow. A current MDCT protocol for CT angiography provides high-resolution arterial phase images from the thoracic inlet to the femoral arteries. This coverage incorporates the entire aorta, as well as the organs of the chest, abdomen, and pelvis. Beyond classifying dissections as involving the ascending (Stanford type A) or descending (type B), CT can demonstrate associated findings critical to patient care such as mediastinal hematoma, pericardial effusions, pseudoaneurysm formation, and active extravasation of contrast from the aorta. Quantitative measurement of aneurysm size, location and relation to branch vessels can be used for planning operative or intravascular repair and for monitoring postprocedure anatomy. The necessity for precise and quantitative measurements with CT has become more critical with the continued advancements in endovascular repair with stent-grafts [10,11].

Computed tomography angiography is less operator-dependent than transesophageal echocardiography, allows complete organ visualization, and is faster and more convenient for patients than magnetic resonance imaging and digital subtraction angiography. The latter issues are especially important with severely ill patients. In the setting of blunt and penetrating trauma, CT of the chest

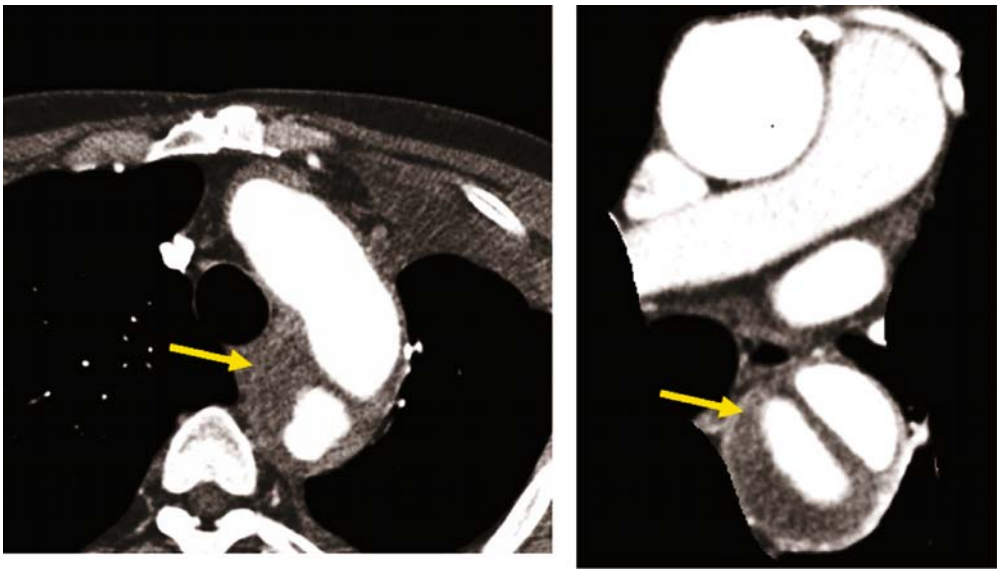

Figure 14.2. Thoracic aortic dissection extending into the transverse aorta (left) and descending thoracic aorta (right). The intramural thrombus is easily identified.

can be extremely useful in diagnosis and as an aid to surgical management [12]. Another major advantage over MR is that these examinations are performed in critically ill patients who may require mechanical ventilation, invasive monitoring, intravenous infusion pumps, and cardiac pacing.

Abdominal Aorta

Aortic aneurysm is associated with risk for sudden death due to aortic dissection or rupture and can occur associated with connective tissue disorders or acquired cardiovascular disease [13]. The ability to measure the diameter, wall thrombus, and calcification makes this an ideal modality for sequential following of patients, and to make an accurate assessment for surgical planning or medical therapy (Figure 14.3). The abdominal aorta is usually scanned before and following intravenous contrast enhancement, which enables detection of calcification of the arterial wall which will be partly obscured following contrast enhancement. It also provides a baseline for evaluating any vascular injury with hemorrhage or thrombus that will be seen on the post-contrast acquisition. Three-dimensional sagittal and coronal reconstructions are routinely performed (Figures 14.4 and 14.5).

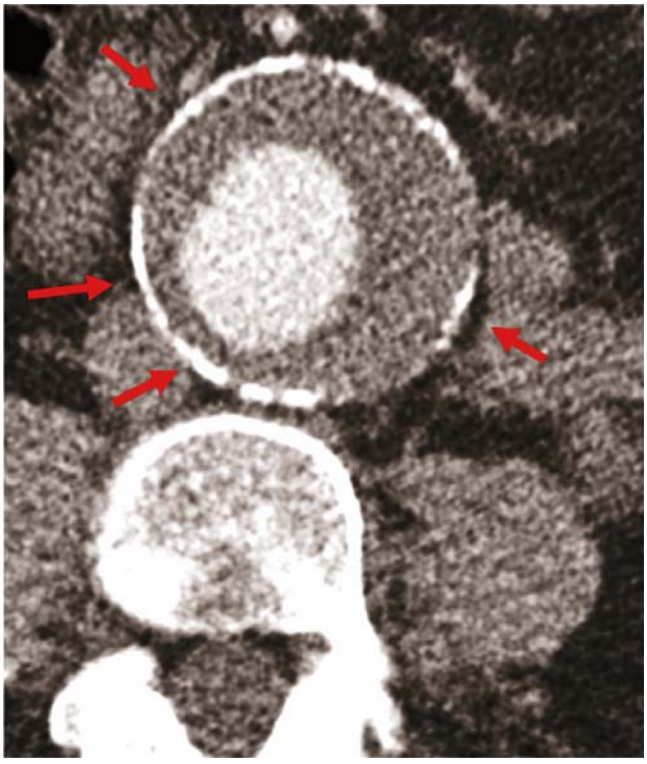

Figure 14.3. Aortic wall calcification and aneurysm on an axial image at the level of the abdominal aorta.

Common Indications for CTA of Abdominal Aorta

1. Detection and depiction of atherosclerotic occlusive disease or aneurysmal dilatation of the abdominal aorta and iliac arteries.
2. Preoperative assessment of aortoiliac aneurysms to determine whether open repair or stent grafting is indicated.
3. Follow-up for the size and progression or regression of abdominal aortic aneurysms.
4. Diagnose the presence and severity of complications following aortic stent-graft placement (leak, pseudoaneurysm, thrombus).
5. Detection and depiction of aortic dissection.
6. Detect the presence of aortic aneurysm rupture.

Accurate measurements of the aortic root diameter can be made easily and the extent of the aneurysm defined. Luminal thrombus is easily identified by differences in tissue density during contrast enhancement. The tomographic format of CT provides excellent definition of the relationship of aortic aneurysms to adjacent structures. Leakage of blood from the aneurysm or stent may be recognizable with contrast enhancement of surrounding tissues.

The two-dimensional images (axial data), maximal intensity projection, and multiplanar imaging allow accurate measurement of length, location, and diameter of aneurysms. The involvement of branch vessels (renals, mesenterics, iliacs, etc.) is also easily assessed with minimal contrast requirements. Computed tomography angiography has become the first-line modality for evaluation for planning stent-graft deployment (Figure 14.5) and post-procedural assessment (Figure 14.6). Cephalocaudal coverage from the celiac trunk to the proximal thighs provides a suitable study volume to detect aortic disease. Although the preoperative assessment requires a true early arterial phase to investigate all preoperative necessities (e.g. aortic neck diameters, angle and distance from the renal arteries), the postoperative study requires a biphasic scan protocol, allowing a more detailed inspection of the perigraft space to rule out possible endoleaks. High-resolution, thin slice protocols are preferable, especially for the post-processing task.

Several studies have demonstrated the accuracy of CT for the diagnosis of aortic diseases. Stueckle et al. compared conventional angiography to CTA in the diagnosis of morphologic changes in the abdominal aorta and its branches in 52 patients who underwent both MDCT and invasive angiography before surgical treatment [14]. All CT examinations were performed after administration of 100 mL contrast medium with a collimation of 4×1 mm and a pitch of 7. All aneurysms, occlusions, stenoses, and calcifications were diagnosed correctly by CTA in axial and multiplanar projections (sensitivity 1.0; specificity 1.0).

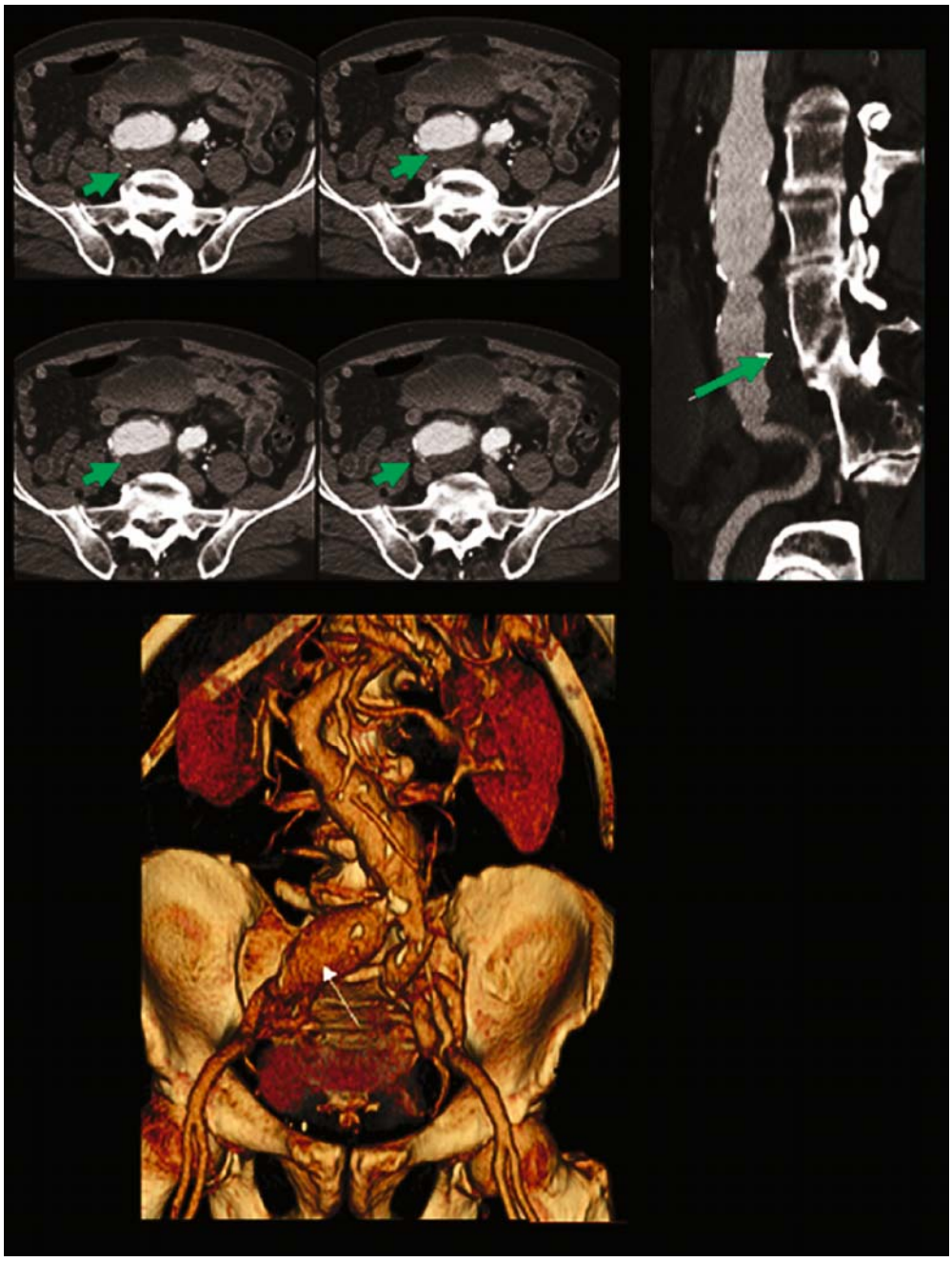

Figure 14.4. A representation of the two-dimensional axial images (top left), curved multiplanar reformat (top right) and volume-rendered images (bottom) of a patient with an abdominal aortic aneurysm. The iliacs and femoral bifurcations can be seen best in their true anatomic three-dimensional orientation with the volume-rendered image. The thrombus, however, is only visible on the two-dimensional images and curved MIP image (green arrows).

The degree of stenosis was overestimated in three cases when using axial projections. Three-dimensional volume-rendered CTA showed a sensitivity of 0.91 for aneurysms, 0.82 for stenoses, 0.75 for occlusions, and 0.77 for calcifications. The specificity was 1.0 in all cases. Multislice CT angiography seems to be similar to invasive angiography for abdominal vessels if multiplanar projections are used.

Nihan et al. described 25 patients (22 preoperative and 3 postoperative) who underwent EBT angiography prior to surgery, with results compared to surgical findings [15]. Among the 22 preoperatively evaluated patients, 17 patients had thoracic and/or abdominal aorta aneurysm with or without associated mural thrombus and calcified arteriosclerotic plaques, and 4 had dissection in the thoracic and abdominal aorta. The findings by CTA correlated with the surgical findings in all cases. In one preoperative patient, interventional angiography resulted in the misdiagnosis of occlusion in the proximal part of the abdominal aorta but EBA showed tortuosity and division anomaly of the abdominal aorta which could not be evaluated by interventional angiography because of technical limitations. There was one postoperative case of a patient with Marfan's syndrome who was found to have a pseudoaneurysm surrounding a graft in the ascending thoracic aorta with contrast extending from the pseudoaneurysmal space to the

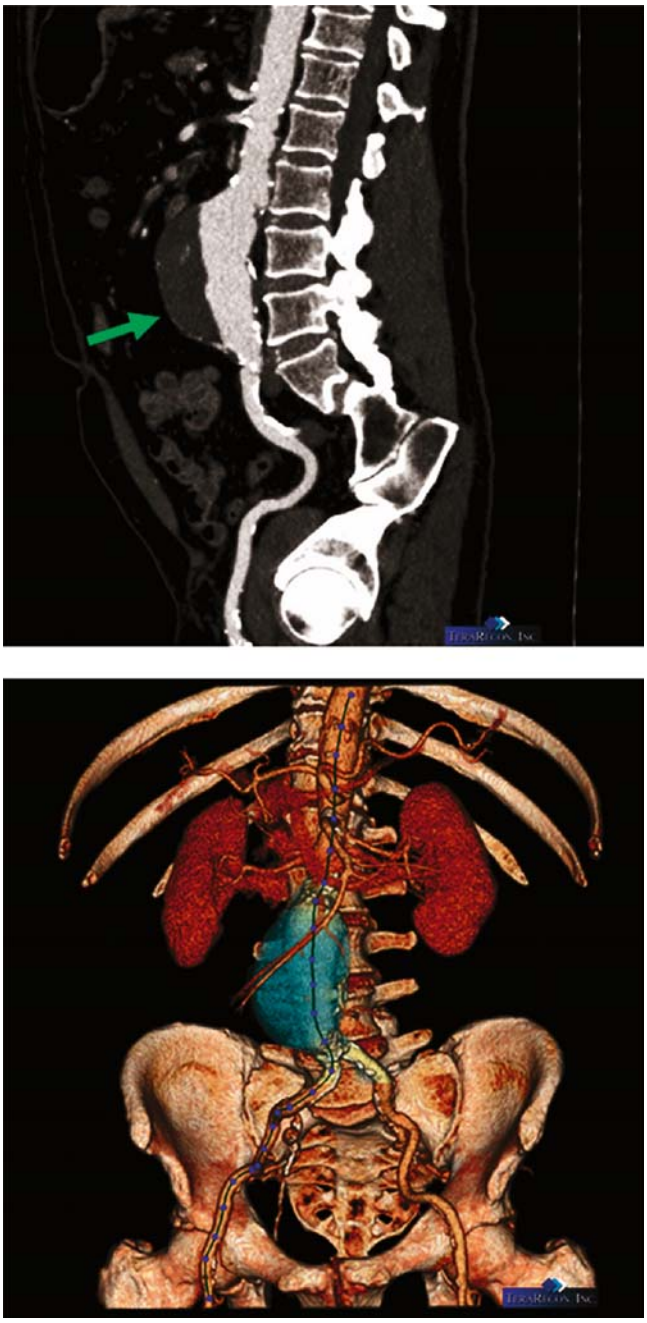

Figure 14.5. Abdominal aortic aneurysm with large intramural thrombus, seen on maximal intensity projection image (top, green arrow) and volume-rendered image (bottom, blue structure). (Courtesy of TeraRecon, Inc.)

right atrium. These findings were in addition to that found on conventional invasive angiography. These findings demonstrated that CTA is a highly accurate imaging method in all kinds of thoracic and abdominal aorta diseases in the preoperative and postoperative period with excellent 3-D images competitive in quality with interventional angiography. In some instances, CT angiography images give more information about the aortic diseases due to visualization of lumen, thrombus, and wall disease simultaneously, as compared to interventional angiography.

Comparison to Other Modalities

Like CT, MRA of the abdomen is always acquired as part of a routine lower extremity runoff procedure most commonly performed for symptoms of claudication.

With CT, the renals can be routinely evaluated during an abdominal aorta study. For MR, the evaluation of the renal arteries for characterizing potential renal artery stenosis in patients with hypertension must be done as a separate procedure, with different imaging protocols. This is also true for evaluation of a potential renal donor. In these patients, dedicated abdominal MRA acquisition is required with greater contrast enhancement, which is not feasible when the legs and feet must also be imaged at the same time. This is because there is a limit on the total volume of gadolinium, which is usually 60–75 mL for an adult. An abdominal MRA performed for the indications listed above is often scanned as part of the same procedure as a thoracic MRA, as it is for CT.

Conclusion

The simultaneous acquisition of multiple thin collimated slices in combination with enhanced gantry rotation speed

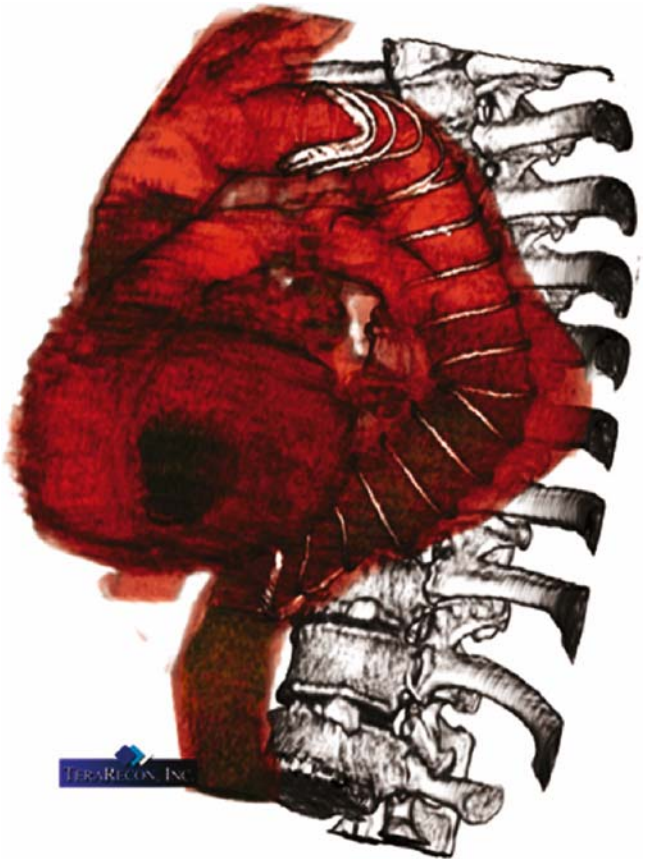

Figure 14.6. A patient status post repair of a thoracic aortic aneurysm. The stent can be seen, without scatter artifact or partial volume effect. (Courtesy of TeraRecon, Inc.)

offers thin slice coverage of extended volumes without any loss in spatial resolution. Using 4-detector-row CT scanners, the scan volume still has to be restricted and focused on dedicated abdominal vessel territories in order to provide high spatial resolution (1–2 mm), while 16-detector-row technology (or greater) now enables full abdominal coverage from the diaphragm to the groin without compromise of spatial resolution. This technique enables the evaluation of the whole arterial visceral vasculature (e.g. hepatic vessels, mesenteric vessels, renal arteries) and the aortic-iliac axis in a single data acquisition.

Renal and Mesenteric Arteries

CTA, combined with abdominal/parenchymal imaging, is a first-line diagnostic test in patients with suspected abdominal vascular emergencies, such as acute mesenteric ischemia, and an excellent tool to assess a wide variety of vascular abnormalities of the abdominal viscera. Important indications for directed renal artery imaging comprise the assessment of patients with suspected renal vascular hypertension to exclude hemodynamically significant renal artery stenosis as well as a complete preoperative assessment for renal transplant candidates. MDCT angiography of the renal arteries is performed with a high-resolution protocol (thickness of 1–1.25 mm or less). Achieving adequate coverage to encompass the entire kidneys and the origins of accessory renal arteries is easily accomplished in a scan of less than 10 seconds duration, or as part of the aortic evaluation (described above). With adequate selection of acquisition parameters (thin collimation) high spatial-resolution volumetric datasets for subsequent 2-D and 3-D reformation can be acquired (Figure 14.7). Whereas fast acquisitions allow a reduction of total contrast volume in the setting of CTA, this is not the case when CTA is combined with a second-phase abdominal MDCT acquisition for parenchymal (e.g. hepatic) imaging. Renal CTA is an accurate and reliable test for visualizing vascular anatomy and renal artery stenosis, and therefore a viable alternative to MRA in the assessment of patients with renovascular hypertension and in potential living related renal donors.

Figure 14.7. A volume-rendered image of the abdominal aorta and vessels (including exquisite detail of the mesenteric and iliac arteries) using 64-detector MDCTA.

Methods

Routine clinical practice follows the rule of thumb that the injection duration should match the acquisition time. Biphasic injection protocols, with an initially high injection rate followed by a slower continuing injection phase, ensure optimal opacification of the renal arteries (Chapter 2). Note that high-concentration contrast material requires only moderate injection flow rates (maximum of 4.5 mL/s) to achieve high iodine administration rates [16].

By using a half-second MDCT scanner and a 1 mm nominal section thickness, Willmann et al. [17] obtained excellent quality CT angiograms (92% and 99% sensitivity and specificity, respectively) for the detection of hemodynamically significant arterial stenosis of aortoiliac and renal arteries. When compared to MR angiography, there is no statistically significant difference between 3-D MR angiography and MDCT angiography in the detection of hemodynamically significant arterial stenosis of the aortoiliac and renal arteries. This study also demonstrated that patient acceptance of the CT study is higher than either invasive angiography or MR angiography.

Tepe et al. used 3-D EBT angiography to evaluate renal artery lesions, as well as vascular variants that it is crucial to detect before surgery [18]. Forty patients underwent EBT (GE-Imatron, C 150 ultrafast CT scanner, San Francisco, CA) of the renal arteries. The study demonstrated that both maximal intensity projection (MIP) and volume-rendered images were excellent in demonstrating stenosis of the renal arteries. Accessory and main renal arteries were easily depicted, and stenosis shown with high accuracy. In this study, among 40 renal angiography patients, 21 had stenosis of the renal arteries with different percentages. A total of 12 accessory renal arteries (5 left, 7 right) were detected. CT, with its non-invasive volume rendering (VR) and MIP techniques, is easy to apply and is functional and accurate for neoplasms, renal vascular anatomy, and renal artery stenosis.

While most vascular beds have demonstrated an advantage of MIP imaging over VR for accurate stenosis detection (especially coronary artery imaging), renal vasculature seems more amenable to quantitation with VR. One study specifically compared overall image quality and vascular delineation on MIP and VR images. The authors

found that all main and accessory renal arteries depicted at invasive angiography were also demonstrated on MIP and VR images [19]. VR performed slightly better than MIP for quantification of stenoses greater than 50% (VR: $r^2 = 0.84$, $p < 0.001$; MIP: $r^2 = 0.38$, $p = 0.001$) and significantly better for severe stenoses (VR: $r^2 = 0.83$, $p < 0.001$; MIP: $r^2 = 0.21$, $p = 0.1$). For detection of stenosis, VR yielded a substantial improvement in positive predictive value (VR: 95% and 90%; MIP: 86% and 68% for stenoses greater than 50% and 70%, respectively). Image quality obtained with VR was not significantly better than that with MIP; however, vascular delineation on VR images was significantly better (Figure 14.8). The VR technique of renal MR angiography enabled more accurate detection and quantification of renal artery stenosis than did MIP, with significantly improved vascular delineation.

Another study evaluated findings in 50 main and 11 accessory renal arteries [20]. All arteries depicted on conventional angiograms were visualized on MIP and VR images. Receiver operating characteristic (ROC) analysis for MIP and VR images demonstrated excellent discrimination for the diagnosis of stenosis of at least 50% (area under the ROC curve, 0.96–0.99). While in this study, sensitivity was not significantly different for VR and MIP (89% versus 94%, $p > 0.1$), specificity was greater with VR (99% versus 87%, $p = 0.008$ to 0.08). Stenosis of at least 50% was overestimated with CT angiography in four accessory renal arteries, but three accessory renal arteries not depicted at conventional angiography were depicted at CT angiography. In the evaluation of renal artery stenosis, CT angiography with VR is faster and more accurate than CT angiography with MIP. Accessory arteries not depicted with conventional angiography were depicted with both CT angiographic algorithms.

Computed tomography angiography is a highly reliable technique for detection of renal artery stenosis as well as for morphologic assessment (Figure 14.8). In patients with renal insufficiency, magnetic resonance angiography or color-coded duplex ultrasound should remain the initial examination performed, depending on local expertise and availability.

Mesenteric Vasculature

MDCT angiography has become a valuable minimally invasive tool for the visualization of normal vascular anatomy and its variants as well as for pathologic conditions affecting the mesenteric vessels (Figures 14.9 to 14.11) [17,21,22]. Indications for MDCT angiography include not only acute and chronic ischemia, aneurysm, and dissection but preoperative vascular assessment for patients undergoing liver lesion embolization as well as in the setting of liver transplantation [23,24]. Protocols for typical aortic imaging (described above) are used to image the mesenteric vasculature. The reconstructed images allow for easy evaluation of all abdominal vasculature. Volume rendering is most often used, predominantly due to the complex anatomy, making MIP imaging more difficult (Figure 14.11). Since the arteries are highly tortuous, leaving the 2-D plane often (and traveling both caudally and cranially at different times), these vessels pose the most challenge with axial interpretations. With coronary imaging, the arteries run cranial to caudal, without significant exception. Thus,

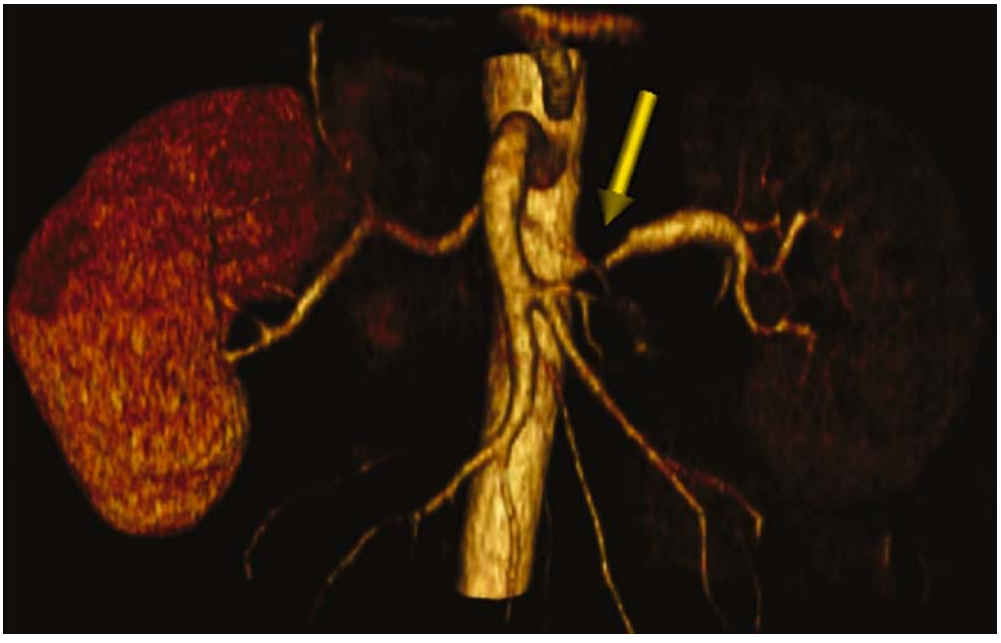

Figure 14.8. A volume-rendered EBT study of the renal arteries, depicting a high-grade stenosis of the left renal artery (arrow). The left kidney also opacifies less (darker color) than the right kidney, suggesting decreased blood flow and significance of the visualized stenosis.

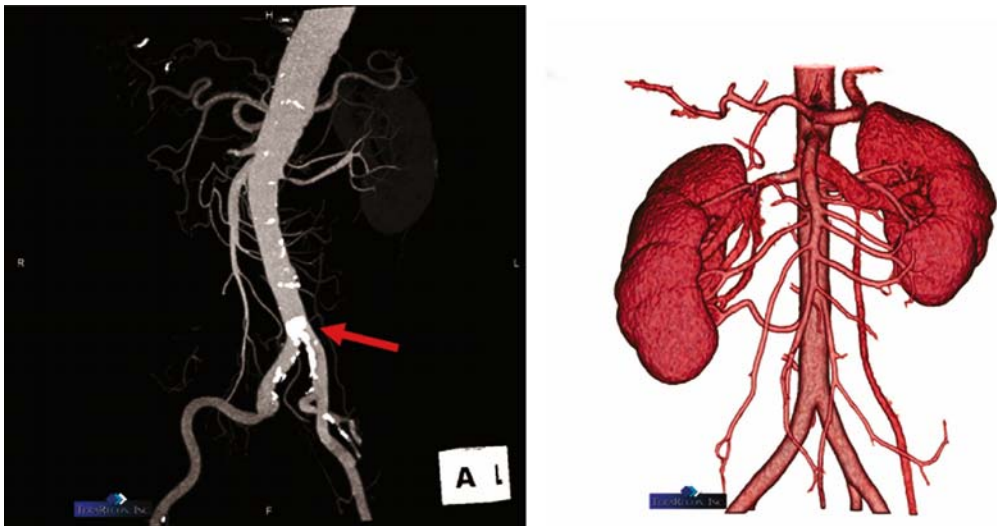

Figure 14.9. Maximal intensity projection of the abdominal aorta, demonstrating severe calcifications at the iliac bifurcation (arrow, left image). The right image demonstrates a normal arterial bed in another patient, displayed using volume rendering. (Courtesy of TeraRecon, Inc.)

interpreting with MIP or axial imaging is fairly straightforward, as the operator needs to systematically go from the most cranial images to the most caudal to follow the respective arteries. With mesenteric imaging, the arteries commonly turn both cranially and caudally, and volume rendering makes visualization of the entire dataset with one reconstruction possible. No studies of the diagnostic potential of the different reconstruction methods have been reported.

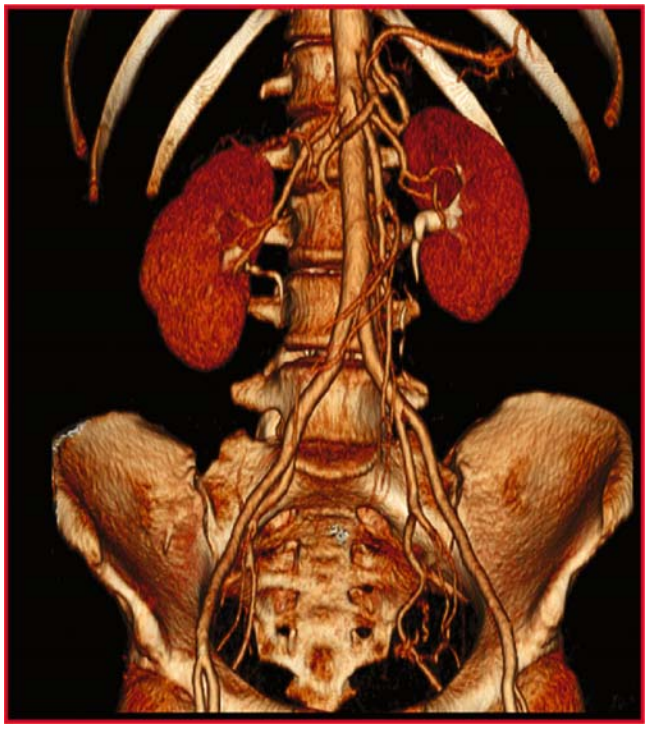

Figure 14.10. A volume-rendered image demonstrating normal renal and mesenteric arteries, as well as aorta and iliac arteries bilaterally. Large volumes of coverage (spanning multiple vascular beds) can be imaged with a single scan.

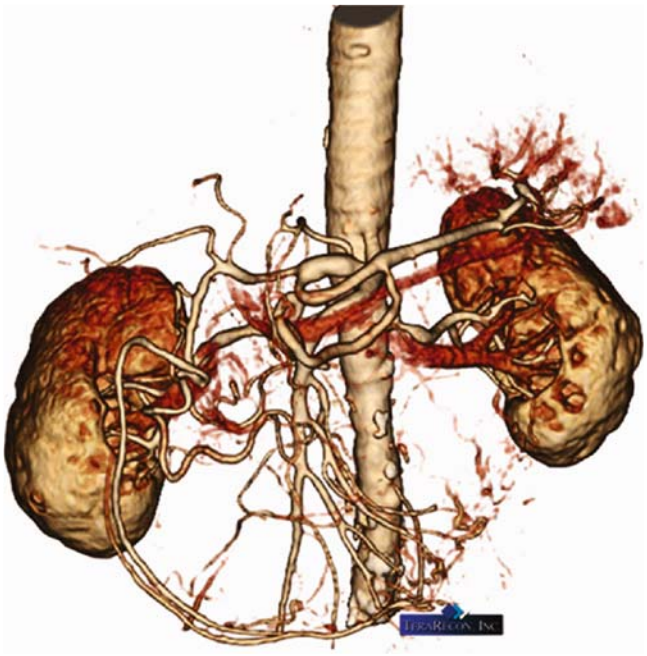

Figure 14.11. Three-dimensional image demonstrating the ability of computed tomography to visualize the abdominal arteries, including the gastric arteries in this case. Reconstruction performed on Aquarius Workstation, TeraRecon, San Mateo, CA. (Courtesy of TeraRecon, Inc.)

Carotid Artery CT Angiography

Ischemic cerebrovascular events are often due to atherosclerotic narrowing of the carotid bifurcation (Figure 14.12) [25]. Invasive angiography is the current reference standard for the evaluation of obstructive carotid artery disease. Computed tomography angiography is a robust technique in assessing carotid artery stenosis, allowing excellent visualization of the lumen of the carotid artery using intravenous contrast (Figure 14.13). Subsequent refinement of magnetic resonance imaging, ultrasound,

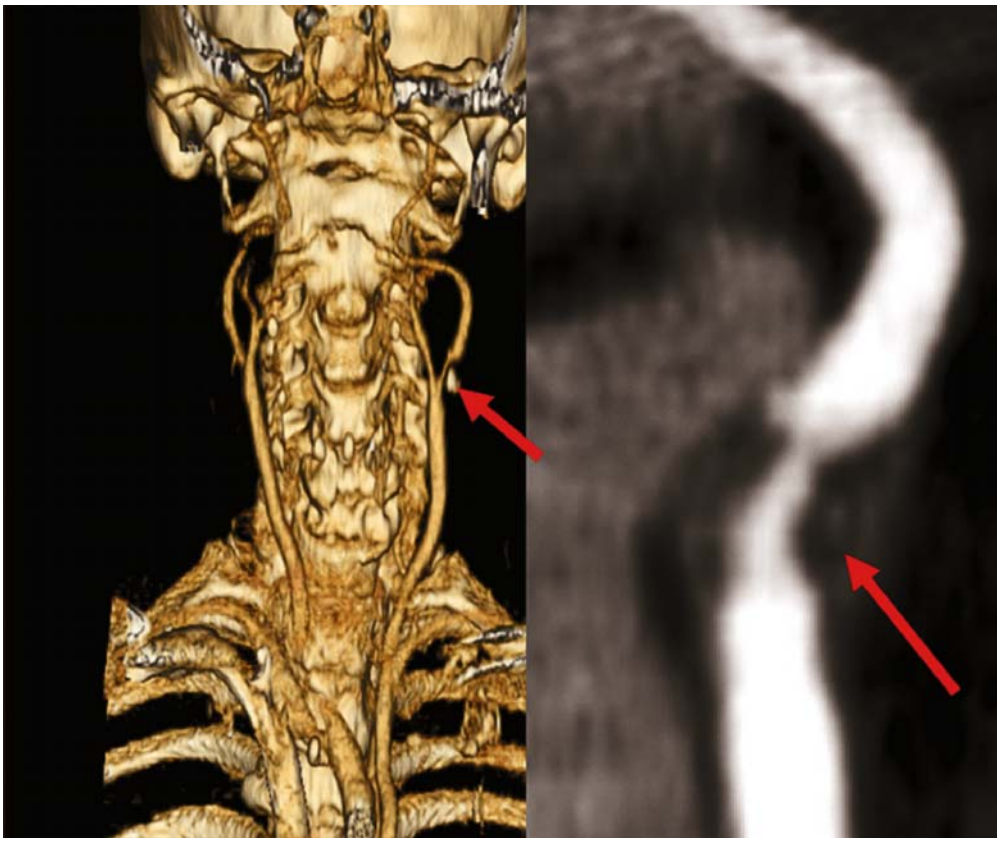

Figure 14.12. Two patients with carotid stenosis at the bifurcation. The left image is a volume-rendered image, with a high-grade stenosis at the proximal portion of the internal carotid, with a dense calcification also seen. The right image demonstrates a maximal intensity projection image of the same region, with a tight stenosis and thrombus present.

and CT techniques has led to changes in clinical practice whereby many centers have now abandoned conventional X-ray angiography in place of safer imaging modalities [26]. Computed tomography angiography offers details of the entire relevant neurovascular axis by excluding significant carotid disease and intracranial disease [27]. Coupling non-contrast-enhanced cranial CT imaging with CT perfusion imaging and CTA of the entire cerebrovascular axis is both safe and feasible [28]. Current practice is to use CTA to facilitate patient triage and provide specific information to rule out large vessel stenosis in patients with transient ischemic attacks, suspected stroke, or in

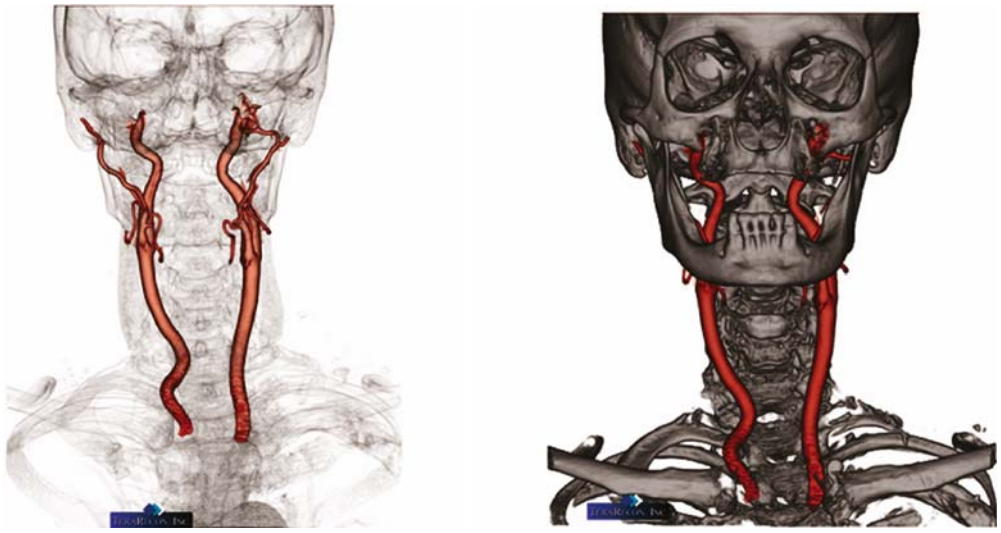

Figure 14.13. Three-dimensional images of normal carotid arteries bilaterally. (Courtesy of TeraRecon, Inc.)

patients with carotid bruits. Furthermore, clarification of equivocal results of carotid ultrasound or MRA is also a common indication. This chapter will address the clinical applications of CT angiography of the carotid and vertebral arteries.

Since treatment has demonstrated a large reduction in strokes by performing carotid endarterectomy [26,29] in symptomatic patients with a stenosis of more than 70%, accurate assessment of carotid disease is important. Furthermore, endarterectomy in patients with a symptomatic moderate carotid stenosis of 50–69% produced a moderate reduction in the risk of stroke [30]. Randoux et al. prospectively compared gadolinium-enhanced magnetic resonance (MR) angiography and computed tomographic (CT) angiography with invasive angiography for use in detecting atheromatous stenosis and plaque morphology at the carotid bifurcation in 22 patients [31]. There was significant correlation between CTA, enhanced MRA, and invasive angiography. Severe internal carotid artery (ICA) stenoses were detected with high sensitivity and specificity: 100% and 100%, respectively, with CT angiography; 93% and 100%, respectively, with enhanced MRA. Luminal surface irregularities and ulcerations were most frequently seen at CTA. Most studies suggest that CT angiography is the best modality for analyzing plaque morphology because it allows visualization of the atheromatous plaque. Detection of ulcerated plaques may prove to be important, since it has been suggested that the presence of plaque ulceration is a risk factor for embolism [32]. However, the inability of invasive angiography to depict plaque ulceration is well documented [33,34], partly because of the limited number of views that are typically obtained. In the case in which CT angiography depicted an ulceration that was not depicted at gadolinium-enhanced MR angiography, this could be due to a lack of spatial resolution at gadolinium-enhanced MR angiography.

CT angiography and gadolinium-enhanced MR angiography have both proved reliable and fast techniques to evaluate the degree of ICA stenosis [34]. CT angiography has some substantial benefits, including its accuracy and lack of invasiveness [35], and improved spatial and temporal resolution as compared with MR angiography.

Methods for Carotid CT Angiography

Carotid CT angiographic images are obtained with patients placed in the supine position with the head tilted back as far as possible to avoid inclusion of dental hardware. Spiral data can be acquired with a 0.5 to 1.5 mm collimation starting at the seventh cervical vertebra and proceeding as far cephalad as possible. Some centers suggest starting at the CT parameters including a field of view (FOV) of 15 × 15 cm and a section thickness of 1 mm. With a power injector, 80–140 mL of non-ionic contrast medium is injected at a rate of 2.5 mL/s into an antecubital vein. Administration of each bolus was followed immediately by a 20 mL saline flush. The acquisition is initiated after the start of the administration of contrast medium, the time of which was determined by a test of circulation time.

EBT scanning for carotid stenosis utilizes the 50 to 100 ms exposure times per slice, using the continuous volume mode and a 10-second breath-hold. The angle of the jaw is angled up, to get the jawbone (and possible associated metal fillings) out of the axial images that include the carotid bifurcation. A total of 60–80 mL of contrast is utilized, injected at a rate of 3 mL/s.

In general, good image quality is essential. A CT angiographic image of good quality is easily obtained if the patient does not move during the study. Given the faster scan times with increased detector systems, this is even easier. A breath-hold acquisition is not necessary. Compared with invasive angiography and CTA, a major limitation of gadolinium-enhanced MR angiography is spatial resolution. By using automatic triggering with detection of the contrast material bolus, it is fairly straightforward to selectively obtain an arterial phase image. Previous studies [36] have shown that a combination of optimal tracking volume placement and adjustment of tracking volume size ensures optimal sensitivity to the contrast material bolus. By choosing a 5 × 20 mm tracker volume placed in the aortic arch, bolus arrival was always detected. Careful timing is very important, with arterial enhancement critical. It is vital to make sure that there is no venous filling when images are obtained. Obtaining images too early will lead to non-enhanced images, and obtaining images late allows for venous enhancement. Large jugular veins filled with contrast in close proximity to the carotid arteries can make the interpretation of carotid arteries more difficult.

Transverse source images are reconstructed in 1 mm increments by using a small FOV (15 cm). These parameters allowed a spatial resolution of 1.0 × 0.3 × 0.3 mm. Total coverage is approximately 18 cm. The images are then analyzed with axial images and maximal intensity projection or curved multiplanar reconstruction. Total post-processing time is approximately 5 minutes per carotid artery. Precision of length and degree of stenosis is reported to depend more on measurement technique than on acquisition parameters [37]. The accuracy of stenosis measurement depends on the scanning plane, which ideally should be perpendicular to the carotid artery used to obtain magnified transverse oblique images. Most authors consider maximal intensity projection or curved multiplanar reconstructions the most accurate techniques for measurements. Volume rendering is considered the least accurate technique for measurement.

Comparison to MR

Gadolinium-enhanced MR angiography is an appropriate technique for evaluating ICA stenosis [38–40]. Clinically relevant stenosis and occlusions of the ICA were correctly

detected with good sensitivity and specificity and good interobserver agreement. Most studies [39,40] with gadolinium-enhanced MR angiography demonstrate overestimation of the degree of stenosis [41]. Artifacts due to excessive section thickness, necessary with current MR systems, cause a partial volume effect [42,43]. The signal loss can also be explained by the presence of hemodynamic modifications. The decreased flow caused by stenosis leads to a reduced concentration of contrast agent in the distal arterial lumen, which may also explain why overestimation of stenosis with gadolinium-enhanced MR angiography can occur [44], especially for evaluating the degree of stenosis in small-vessel lumens.

Plaques that are more prone to disruption, fracture, or fissuring may be associated with a higher risk of embolization, occlusion, and consequent ischemic neurologic events [45]. Plaque irregularities are more frequent at CT angiography than at invasive angiography or contrast-enhanced MR angiography.

In general, studies demonstrate that MR angiography sometimes performs inferiorly to CT angiography, mainly due to lower spatial resolution. MR has been postulated to demonstrate inflammation, and MRI-derived measurements of fibrous-cap and lipid-core thickness have the potential for identifying vulnerable carotid plaques in vivo, although this application is still very experimental [46]. CT does not have the same potential for demonstrating flow or inflammation.

Invasive angiography has long been considered the standard for evaluation of carotid stenosis but has well-known risks and limitations. Invasive angiography allows only a limited number of views, which can lead to an underestimation of the degree of stenosis by as much as 40% [47] when compared with histologic correlation. Invasive angiography is also a relatively expensive technique that uses numerous resources. Finally and perhaps most importantly, there is a small but definite risk of major complications secondary to the procedure itself. The Asymptomatic Carotid Atherosclerosis Study Committee reported a 1.2% risk of persisting neurologic deficit or death following invasive angiography, while the surgical risk was 1.5%. The risks associated with CT angiography are markedly lower with similar or lower radiation exposures and no catheter-induced risks.

Almost all authors consider that calcified plaque is a limitation of CT angiography. This can be minimized when multiplanar volume reconstruction is used, although circumferential calcified plaques will still cause problems. Carotid arteries tend to calcify less than either coronary or peripheral arteries (perhaps due to the fact that carotid arteries are more elastic and less muscular), so dense circumferential calcifications occur less frequently in this vascular bed.

CTA has been shown to have a pooled sensitivity of 95% and specificity of 98% for the detection of >70% stenoses, even if only older scanners are used. Differentiation between lipid, fibrous, and calcified plaques may be possible, especially with e-Speed EBT scanning. Carotid CTA has come of age and can be used to quantify stenoses more precisely than ultrasound, to detect tandem stenoses and for the workup of acute stroke patients. The e-Speed EBT scanner has the additional advantage of a very low radiation profile, allowing for minimal risk to the patient, and maximum visualization of the arteries in question.

Imaging the Vertebral Artery

Although conventional intra-arterial angiography remains the gold standard method for imaging the vertebral artery, non-invasive modalities such as ultrasound, multislice computed tomographic angiography and magnetic resonance angiography are constantly improving and are playing an increasingly important role in diagnosing vertebral artery pathology in clinical practice. Normal anatomy, normal variants, and a number of pathologic entities such as vertebral atherosclerosis, arterial dissection, arteriovenous fistula, subclavian steal syndrome, and vertebrobasilar dolichoectasia can be seen.

Summary

During the past decade, we have been witness to a tremendous development in the field of CT imaging. CTA has gained remarkably by improvements in scan time and image quality, replacing diagnostic angiography in many cases of peripheral, carotid, and renal angiography. These vascular beds do not suffer from motion artifacts, so imaging with CT is ideal. CTA is less expensive, less invasive, and allows simultaneous visualization of large anatomic areas from multiple angles using 3-D display. Nevertheless, along with exciting advances, MDCT also carries some emerging and important issues such as increased patient radiation exposure and continued exposure to iodinated contrast.

References

1. Rooholamini SA, Stanford W: Ultrafast computed tomography in the diagnosis of aortic aneurysms and dissections. In: Stanford W, Rumberger J (eds) Ultrafast computed tomography in cardiac imaging: principles and practice. Mount Kisco, NY: Futura Publishing, 1992: 287–310.
2. Katz DS, Hon M. CT angiography of the lower extremities and aortoiliac system with a multi-detector row helical CT scanner: promise of new opportunities fulfilled. Radiology 2001;221:7–10.
3. Kim JK, Park SY, Kim HJ, et al. Living donor kidneys: usefulness of multi-detector row CT for comprehensive evaluation. Radiology 2003;229:869–876.
4. Fishman JE. Imaging of blunt aortic and great vessel trauma. J Thorac Imaging 2000;15(2):97–103.
5. Kouchoukos NT, Dougenis D. Surgery of the thoracic aorta. N Engl J Med 1997;336(26):1876–1888.
6. Rubin GD. Helical CT angiography of the thoracic aorta. J Thorac Imaging 1997;12(2):128–149.

7. Rubin GD, Shiau MC, Leung AN, Kee ST, Logan LJ, Sofilos MC. Aorta and iliac arteries: single versus multiple detector-row helical CT angiography. Radiology 2000;215(3):670–676.
8. Gotway MB, Dawn SK. Thoracic aorta imaging with multislice CT. Radiol Clin North Am 2003;41:521–543.
9. Roos JE, Willmann JK, Weishaupt D, et al. Thoracic aorta: motion artifact reduction with retrospective and prospective electrocardiography assisted multi-detector row CT. Radiology 2002;222:271–277.
10. Galla JD, Ergin MA, Lansman SL, et al. Identification of risk factors in patients undergoing thoracoabdominal aneurysm repair. J Cardiac Surg 1997;12:292–299.
11. Semba CP, Kato N, Kee ST, et al. Acute rupture of the descending thoracic aorta: repair with use of endovascular stent-grafts. J Vascular Intervent Rad 1997;8(3):337–342.
12. Zinck SE, Primack SL. Radiographic and CT findings in blunt chest trauma. J Thorac Imaging 2000;15(2):87–96.
13. Lu B, Dai RP, Jing BL, et al. Electron beam tomography with three-dimensional reconstruction in the diagnosis of aortic diseases. J Cardiovasc Surg 2000;41:659–668.
14. Stueckle CA, Haegele KF, Jendreck M, et al. Multislice computed tomography angiography of the abdominal arteries: comparison between computed tomography angiography and digital subtraction angiography findings in 52 cases. Australas Radiol 2004;48(2):142–147.
15. Nihan E, Levent A, Sekup A. Assessment of aortic diseases with electron beam tomographic angiography. EBT Symposium 2003;11–15.
16. Fleischmann D. Multiple detector-row CT angiography of the renal and mesenteric vessels. Eur J Radiol 2003;45(Suppl 1):S79–S87.
17. Willmann JK, Wildermuth S, Pfammatter T, et al. Aortoiliac and renal arteries: prospective intraindividual comparison of contrast-enhanced three-dimensional MR angiography and multi-detector row CT angiography. Radiology 2003;226:798–811.
18. Tepe SM, Memisoglu E, Kural AR. Three-dimensional noninvasive contrast-enhanced electron beam tomography angiography of the kidneys: adjunctive use in medical and surgical management. Clin Imaging 2004;28(1):52–58.
19. Mallouhi A, Schocke M, Judmaier W, et al. 3D MR angiography of renal arteries: comparison of volume rendering and maximum intensity projection algorithms. Radiology. 2002;223(2):509–516.
20. Johnson PT, Halpern EJ, Kuszyk BS, et al. Renal artery stenosis: CT angiography – comparison of real-time volume-rendering and maximum intensity projection algorithms. Radiology 1999 May; 211(2):337–343.
21. Laghi A, Iannaccone R, Catalano C, et al. Multislice spiral computed tomography angiography of mesenteric arteries. Lancet 2001;358: 638–639.
22. Lawler LP, Fishman EK. Celiomesenteric anomaly demonstration by multidetector CT and volume rendering. J Comput Assist Tomogr 2001;25:802–804.
23. Erbay N, Raptopoulos V, Pomfret EA, et al. Living donor liver transplantation in adults: vascular variants important in surgical planning for donors and recipients. Am J Roentgenol 2003;181:109–114.
24. Byun JH, Kim TK, Lee SS, et al. Evaluation of the hepatic artery in potential donors for living donor liver transplantation by computed tomography angiography using multidetector-row computed tomography: comparison of volume rendering and maximum intensity projection techniques. J Comput Assist Tomogr 2003;27: 125–131.
25. Kannel WB. Current status of the epidemiology of brain infarction associated with occlusive arterial disease. Stroke 1971;2:295–318.
26. North American Symptomatic Carotid Endarterectomy Trial Collaborators. Beneficial effect of carotid endarterectomy in symptomatic patients with high-grade carotid stenosis. N Engl J Med 1991; 325:445–453.
27. Smith WS, Roberts HC, Chuang NA, et al. Safety and feasibility of a CT protocol for acute stroke: combined CT, CT angiography, and CT perfusion imaging in 53 consecutive patients. Am J Neuroradiol 2003;24:688–690.
28. Na DG, Ryoo JW, Lee KH, et al. Multiphasic perfusion computed tomography in hyperacute ischemic stroke: comparison with diffusion and perfusion magnetic resonance imaging. J Comput Assist Tomogr 2003;27:194–206.
29. Collaborative Group. MRC European Carotid Surgery Trial: interim results for symptomatic patients with severe (70–99%) or with mild (0–29%) carotid stenosis – European Carotid Surgery Trialists. Lancet 1991;337:1235–1243.
30. Barnett HJ, Taylor DW, Eliasziw M, et al. Benefit of carotid endarterectomy in patients with symptomatic moderate or severe stenosis: North American Symptomatic Carotid Endarterectomy Trial Collaborators. N Engl J Med 1998;339:1415–1425.
31. Randoux B, Marro B, Koskas F, et al. Carotid artery stenosis: prospective comparison of CT, three-dimensional gadolinium-enhanced MR, and conventional angiography. Radiology. 2001;220(1):179–185.
32. Hatsukami TS, Ferguson MS, Beach KW, et al. Carotid plaque morphology and clinical events. Stroke 1997;28:95–100.
33. Comerota AJ, Katz ML, White JV, Grosh JD. The preoperative diagnosis of the ulcerated carotid atheroma. J Vasc Surg 1990;11:505–510.
34. Runge VM, Kirsch JE, Lee C. Contrast-enhanced MR angiography. J Magn Reson Imaging 1993;3:233–239.
35. Marro B, Zouaoui A, Koskas F, et al. Computerized tomographic angiography scan following carotid endarterectomy. Ann Vasc Surg 1998;12:451–456.
36. Castillo M, Wilson JD. CT angiography of the common carotid artery bifurcation: comparison between two techniques and conventional angiography. Neuroradiology 1994;36:602–604.
37. Cinat M, Lane CT, Pham H, Lee A, Wilson SE, Gordon I. Helical CT angiography in the preoperative evaluation of carotid artery stenosis. J Vasc Surg 1998;28:290–300.
38. Leclerc X, Martinat P, Godefroy O, et al. Contrast-enhanced three-dimensional fast imaging with steady-state precession (FISP) MR angiography of supraaortic vessels: preliminary results. Am J Neuroradiol 1998;19:1405–1413.
39. Slosman F, Stolpen AH, Lexa FJ, et al. Extracranial atherosclerotic carotid artery disease: evaluation of non-breath-hold three-dimensional gadolinium-enhanced MR angiography. Am J Roentgenol 1998;170:489–495.
40. Scarabino T, Carriero A, Magarelli N, et al. MR angiography in carotid stenosis: a comparison of three techniques. Eur J Radiol 1998;28:117–125.
41. Cronqvist M, Stahlberg F, Larsson EM, Lonntoft M, Holtas S. Evaluation of time-of-flight and phase-contrast MRA sequences at 1.0 T for diagnosis of carotid artery disease. I. A phantom and volunteer study. Acta Radiol 1996;37:267–277.
42. Remonda L, Heid O, Schroth G. Carotid artery stenosis, occlusion, and pseudo-occlusion: first-pass, gadolinium-enhanced, three-dimensional MR angiography – preliminary study. Radiology 1998; 208:95–102.
43. Levy RA, Prince MR. Arterial-phase three-dimensional contrast-enhanced MR angiography of the carotid arteries. Am J Roentgenol 1996;167:211–215.
44. Evans AJ, Richardson DB, Tien R, et al. Poststenotic signal loss in MR angiography: effects of echo time, flow compensation, and fractional echo. Am J Neuroradiol 1993;14:721–729.
45. Eliasziw M, Streifler JY, Fox AJ, Hachinski VC, Ferguson GG, Barnett HJ. Significance of plaque ulceration in symptomatic patients with high-grade carotid stenosis: North American Symptomatic Carotid Endarterectomy Trial. Stroke 1994;25:304–308.
46. Fayad ZA, Sirol M, Nikolaou K, Choudhury RP, Fuster V. Magnetic resonance imaging and computed tomography in assessment of atherosclerotic plaque. Curr Atheroscler Rep 2004;6(3):232–242.
47. Ho VB, Foo TK. Optimization of gadolinium-enhanced magnetic resonance angiography using an automated bolus-detection algorithm. Invest Radiol 1998;33:515–523.